

Experimental studies of 1.5–1.6 μm high-power asymmetric-waveguide single-mode lasers

P.V. Gorlachuk, A.V. Ivanov, V.D. Kurnosov, K.V. Kurnosov, A.A. Marmalyuk, V.I. Romantsevich, V.A. Simakov, R.V. Chernov

Abstract. The current–voltage, power–current, and spectral characteristics of high-power single-mode semiconductor lasers emitting at wavelengths of 1.5–1.6 μm are studied experimentally. It is shown that a laser with a cavity length of 1.6 mm and a mesa-stripe width of 3 μm mounted in a housing 11 mm in diameter may emit a power higher than 300 mW. Mounting of lasers on C-mounts makes it possible to achieve powers exceeding 400 mW. In the case of mounting in standard 14 pin DIL packages, the laser power at the exit of a single-mode fibre-optic cable (FOC) was no lower than 100 mW, which, taking into account 50% losses upon radiation coupling into the FOC, corresponds to the laser diode power higher than 200 mW. It is shown that the differential resistance of a laser depends not only on the laser crystal length but also on the type of mounting (in copper housings 11 mm in diameter or on C-mounts). The dependences of the laser wavelength and spectral width on the pump current and ambient temperature are presented. The characteristic temperatures of laser diodes are determined.

Keywords: mesa-stripe structure, high-power laser diode, single-mode lasing, laser diode characteristics, radiation spectral width.

1. Introduction

At present, interest has increased in high-power laser diodes (LDs) emitting in the wavelength range of 1.4–1.6 μm . First of all, this is related to their application in fibre-optic communication lines and as pump sources for erbium-doped fibre-optic amplifiers and Raman fibre amplifiers operating in the wavelength range of 1.4–1.6 μm . These applications require the following LD parameters: stable output power at a level of hundreds of milliwatts, stable peak wavelength, and high radiative efficiency, as well as efficient coupling of the LD radiation into a single-mode optical fibre. High-power semiconductor lasers have found wide application in medicine, environmental monitoring systems, and systems of industrial gas detection. It is agreed that radiation within the wavelength range of 1.5–1.6 μm is eye safe.

Leshko et al. [1] reported the development of high-power single-mode LDs based on InGaAsP/InP quantum-well heterostructures (HSs) ($\lambda = 1.3–1.6 \mu\text{m}$). The InGaAsP/InP separate-confinement heterostructure with a step waveguide, a

threshold current density of 180 A cm^{-2} , and an internal quantum yield of stimulated emission of 93%–99% was grown by the MOCVD method. The mesa-stripe structure for the laser diode based on the developed InGaAsP/InP heterostructure was optimised to achieve the maximum single-mode laser power. The output cw single-mode power of a laser diode with a mesa-stripe width $W = 4.5 \mu\text{m}$ was 185 mW ($\lambda = 1480 \text{ nm}$), while the maximum power reached 300 mW. The external differential quantum efficiency of an LD with a cavity length $L = 1–1.5 \text{ mm}$ was 0.47–0.57 W A^{-1} .

In [2], it was noted that it is impossible to optimise HS parameters to achieve simultaneously the maximum working power and the minimum threshold current. The AlInGaAs/InP separate-confinement heterostructures for wavelengths of 1.2–1.5 μm with four and six quantum wells (QWs) were grown by the MOCVD method. The absolute threshold current reached 10 mA for an LD with a mesa-stripe width $W = 4.5 \mu\text{m}$ and a cavity length of 200 μm . The threshold current densities were 500–600 A cm^{-2} at a cavity length of 1.0 mm. The possibility of cw lasing at an ambient temperature of 170°C without forced cooling was demonstrated. In the temperature range of 10–80°C, the characteristic parameter T_0 reached 110 K. It was shown that the maximum cw power of an LD based on a four-QW heterostructure with a cavity length $L = 1120 \mu\text{m}$ (at reflectivities of the highly reflecting and output mirrors of 95% and 5%, respectively) and a pump current of 1400 mA was 300 mW, and this was not a limiting value.

The influence of the number of QWs in the active region on the linearity of the power–current ($P-I$) characteristic of a semiconductor laser was considered in [3]. It was shown that the use of two QWs as an active region leads to a considerable increase in the internal quantum efficiency of stimulated emission and to a considerably better linearity of the laser $P-I$ in comparison with a single-well structure. At the same time, the use of three and more QWs leads only to a slight increase in the power characteristics in comparison with a two-well structure. Thus, the two-well structure, taking into account the simplicity of its growth, is optimal for obtaining high output powers.

Lysevych et al. [4] considered the influence of the QW position inside a 1- μm laser structure on the output power. Characteristics of three heterostructures were studied. The QW lied in the centre of the first laser structure, was shifted by 300 nm to the adjacent n-layer in the second HS, and shifted by 300 nm to the p-emitter in the third HS. It was shown that the maximum output power in the case of the third HS was 25% higher than in the first two cases.

For development of high-power LDs, asymmetric heterostructures with a superwide (wider than 1 μm) waveguide are

P.V. Gorlachuk, A.V. Ivanov, V.D. Kurnosov, K.V. Kurnosov, A.A. Marmalyuk, V.I. Romantsevich, V.A. Simakov, R.V. Chernov Open Joint-Stock Company M.F. Stel'makh Polyus Research Institute, ul. Vvedenskogo 3, stroenie 1, 117342 Moscow, Russia; e-mail: webeks@mail.ru

Received 5 February 2018; revision received 9 April 2018

Kvantovaya Elektronika 48 (6) 495–501 (2018)

Translated by M.N. Basieva

used most widely. Studies on high-power LDs are reviewed in [5]. The influence of asymmetric position of the active LD region in a superwide waveguide on the suppression of higher-order modes was considered in [6]. The active region for a waveguide 1.7 μm thick should be shifted by 0.2 μm to the p-emitter; in this case, the thicknesses of the p- and n-waveguides become 0.65 and 1.05 μm , respectively [6–8].

Works [9, 10] were devoted to the development of LDs with a maximum output power and a maximum working temperature. Structures with asymmetric waveguides were theoretically studied in [11, 12].

In the case of a mesa-stripe width of 100 μm , one may neglect the broadening of the LD active region due to spreading of the pump current over the p-waveguide. However, this broadening of the active region in single-mode LDs with a stripe width of 2–5 μm is inadmissible.

In the present work, we experimentally study high-power single-mode lasers ($\lambda = 1.5\text{--}1.6 \mu\text{m}$) with asymmetric waveguides. The distinction of these lasers from the previously studied lasers with asymmetric waveguides [6–8] is that the active region in these LDs can be positioned closer to the heat sink due to a considerable decrease in the p-waveguide thickness (to 0.01 μm instead of 0.65 μm). This ensures more efficient heat removal from the LD active region, decreases the emitting region dimension along the p–n junction due to a decrease in the lateral spreading of the pump current over the p-waveguide, and provides single-mode lasing. An increase in the output power is achieved due to an increase in the n-waveguide thickness, because the losses due to free carriers in the n-waveguide are much lower than in the p-waveguide.

2. Parameters of studied heterostructures and lasers on their basis

The heterostructures were grown by the MOCVD method in the $\text{In}_{1-x-y}\text{Ga}_y\text{Al}_x\text{As}/\text{InP}$ system. We grew two QWs, each 70 \AA thick. A barrier layer 120 \AA thick was sandwiched between the QWs; waveguiding layers were positioned to the right and left from the QWs and were 0.01 μm thick on the side of the p-waveguide and 0.73 μm thick on the side of the n-waveguide. The thicknesses of barrier layers were 0.1 μm . In the p-InP emitter, a four-component stop layer with a thickness of 0.012 μm was grown to stop chemical etching of the HS in the process of LD fabrication. The active regions and waveguiding layers were undoped. The grown heterostructure was similar in the geometry of layers and composition to the type-2 heterostructure in [13, Table 2] but had a different p-waveguide thickness (0.01 μm instead of 0.73 μm) and a stop layer.

This structure was used to fabricate mesa-stripe LDs with a stripe width of 3 μm . ZnSe was used for isolation. We studied lasers with cavity lengths of 1.0, 1.6, and 2.2 mm. The cavity faces were coated with reflecting and antireflecting films with reflectivities of about 100% and 5%, respectively. The LD characteristics were measured from the cavity face with the 5% reflectivity.

The laser diodes were mounted in copper housings 11 mm in diameter and on C-mounts. The contact plates and C-mounts were metallised using identical techniques. The laser diodes were soldered with indium with the active regions down. The plate with the LD was placed into a cylindrical housing with a diameter of 11 mm. The housing was mounted on a heat sink, whose temperature was kept constant using an electronic stabilisation circuit at 20, 30, and 40 $^\circ\text{C}$ ($T = T_0 + \Delta T$,

where $T_0 = 20^\circ\text{C}$ and $\Delta T = 0, 10, \text{ and } 20^\circ\text{C}$). The characteristics of the LDs on C-mounts were measured on another setup, the electronic circuit of which maintained temperature at 20 $^\circ\text{C}$. The current–voltage (I – V) and P – I characteristics of laser diodes at a constant pump current were measured at these fixed temperatures.

2.1. Current–voltage and power–current characteristics of LDs

The current–voltage and power–current characteristics of LDs at different heat-sink temperatures are shown in Figs 1 and 2 for cavity lengths of 1.0 and 1.6 mm, respectively.

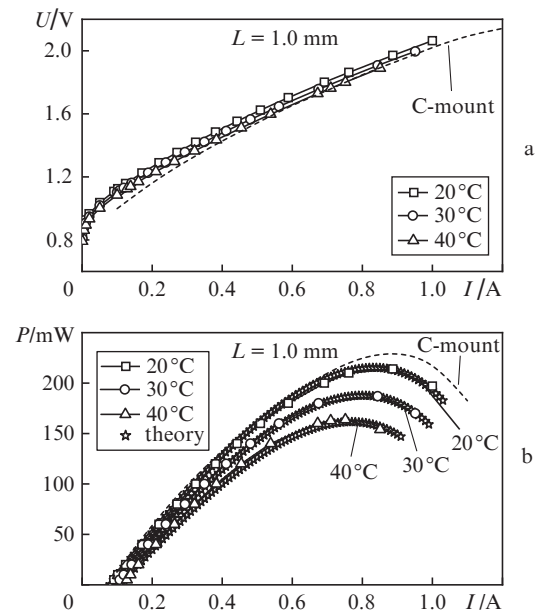


Figure 1. Experimental (a) current–voltage and (b) power–current characteristics of LDs with a cavity length of 1 mm mounted (solid curves) in copper housings 11 mm in diameter and (dashed curves) on C-mounts. Theoretically calculated curves are indicated by asterisks.

Analysis of the I – V characteristics shows that the voltage drop across LDs mounted on C-mounts is lower than the voltage drop across LDs in copper housings, i.e., at identical pump currents, the scattered electric power will be lower and the output power will be higher in the case of C-mounts, which is also confirmed by the P – I characteristics.

For LDs in copper housings with a cavity length $L = 1$ mm, radiation power P exceeding 200 mW can be achieved at a temperature of 20 $^\circ\text{C}$ and pump currents exceeding 700 mA ($P = 215$ mW at a pump current of 880 mA), while LDs with $L = 1.6$ mm have a power of 300 mW at the same temperature at pump currents exceeding 1200 mA.

The output power of LDs on C-mounts reaches 230 mW at a current of 900 mA in the case of $L = 1$ mm, while the 400-mW power of LDs with $L = 1.6$ mm can be achieved at pump currents $I > 1500$ mA.

Comparison of the P – I characteristics shown in Figs 1b and 2b shows that the output power for LDs on C-mounts with a cavity length of 1.6 mm increases with increasing pump current faster than for LDs with a cavity length of 1.0 mm.

In this work, we do not present the I – V and P – I characteristics for diodes with a cavity length of 2.2 mm because

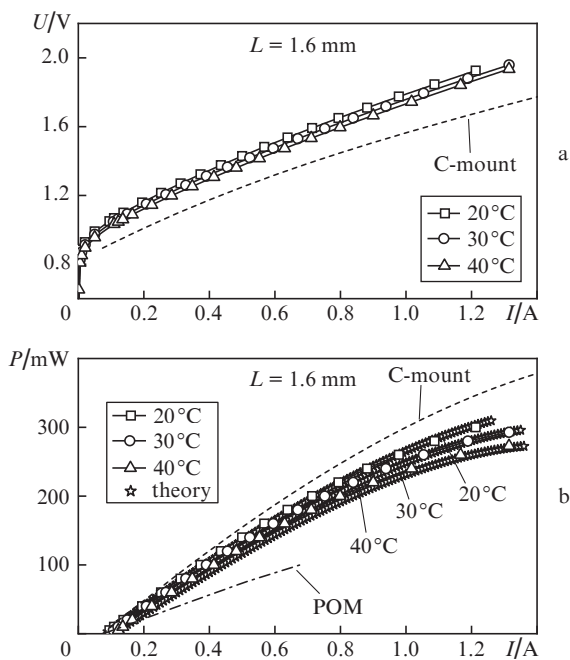


Figure 2. Experimental (a) current–voltage and (b) power–current characteristics of LDs with a cavity length of 1.6 mm mounted (solid curves) in copper housings 11 mm in diameter and (dashed curves) on C-mounts. Theoretically calculated curves are indicated by asterisks. The dot-and-dash curve corresponds to radiation at the exit of the single-mode fibre-optic cable of the optical transmitting module (POM).

they are similar to the characteristics for LDs with a cavity length of 1.6 mm.

For LDs with a cavity length of 2.2 mm, a power of 300 mW can be achieved at a temperature of 20°C and pump currents exceeding 1450 mA. The power of LDs on C-mounts reaches 420 mW at pump currents exceeding 1700 mA. At identical pump currents, the power of a laser with a cavity length of 2.2 mm is lower than the power of a laser with a cavity length of 1.6 mm. However, the P – I characteristic for LDs with a cavity length of 2.2 mm levels off at higher output powers than for LDs with a cavity length of 1.6 mm.

Thus, LDs on C-mount demonstrate a lower voltage drop and a higher output power than LDs in 11-mm-diameter copper housings. The optimal cavity length for LDs with output powers not exceeding 300 mW is 1.6 mm.

2.2. Differential resistance and differential efficiency

Figure 3 presents the dependence of the LD differential resistance ($R_g = \Delta U / \Delta I$, i.e., ratio between the voltage and current increments) on the pump current I for LDs with cavity lengths of (a) 1.0 and (b) 1.6 mm. The ΔU , ΔI , and I parameters were determined as $\Delta U = U_{i+1} - U_i$, $\Delta I = I_{i+1} - I_i$, and $I = (I_{i+1} + I_i) / 2$, where U_{i+1} , U_i , I_{i+1} , and I_i are the experimentally measured voltage and pump currents at the $(i + 1)$ -th and i -th steps.

One can see that the absolute values of the differential resistances of LDs with a cavity length of 1.6 mm are lower than those of LDs with a cavity length of 1.0 mm.

The differential resistance of LDs with a cavity length of 1.0 mm in copper housings is lower than that of LD diodes on C-mounts (the dashed line above the solid curves at $I < 800$ mA). In contrast, LDs with a cavity length of 1.6 mm

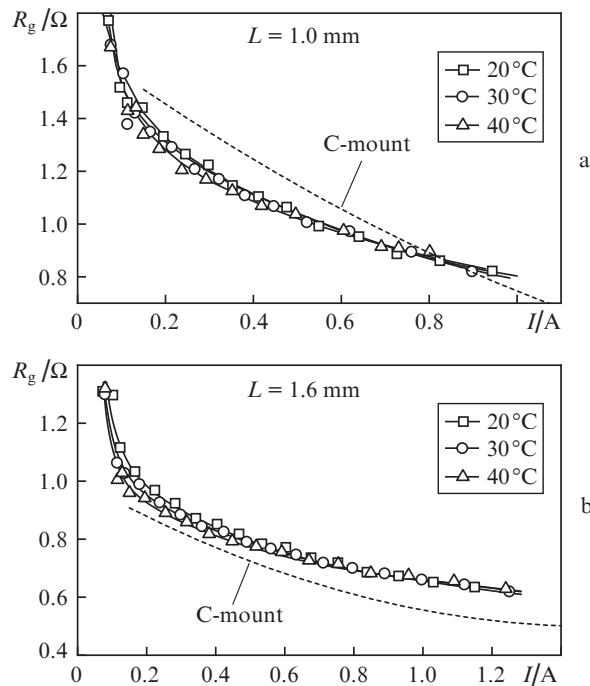


Figure 3. Experimental dependences of the differential resistance on the pump current for LDs with cavity lengths of (a) 1 and (b) 1.6 mm mounted in copper housings (at heat sink temperatures of 20, 30, and 40°C) and (dashed curves) on C-mounts.

in copper housings have a higher differential resistance than LDs on C-mounts.

The differential resistance of LDs with a cavity length of 2.2 mm in copper housings at pump currents below 600 mA almost

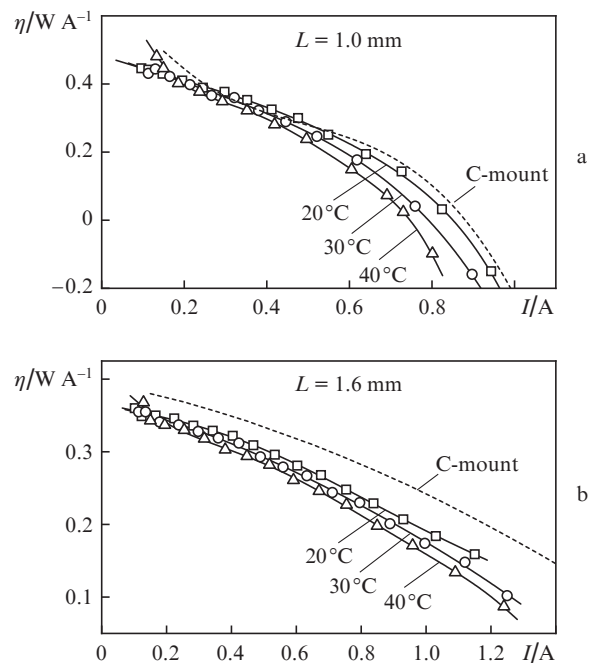


Figure 4. Experimental dependences of the power–current efficiency on the pump current for LDs with cavity lengths of (a) 1 and (b) 1.6 mm mounted (solid curves) in copper housings and (dashed curves) on C-mounts.

coincides with the differential resistance of LDs on C-mounts. At pump currents exceeding 600 mA, the differential resistance of LDs on C-mounts is lower than that of LDs in copper housings.

It was shown in [14] that the differential resistance only slightly affects the laser threshold and efficiency but strongly influences the maximum output power. In other words, the lower the differential resistance, the higher the maximum laser power. A similar conclusion can be made based on the results of our work.

Figure 4 shows the dependences of the differential power–current efficiency ($\eta = \Delta P/\Delta I$, ratio between the output power and pump current increments) on the pump current for LDs with cavity lengths of 1.0 and 1.6 mm mounted in copper housings (solid curves) and on C-mounts (dashed curves). One can see that the power–current efficiency for the LDs on C-mounts is higher than that for LDs in copper housings (this is especially pronounced for LDs with a cavity length of 1.6 mm). Thus, mounting of LDs on C-mounts leads to an increase in the differential efficiency and output power in comparison with LDs in copper housings.

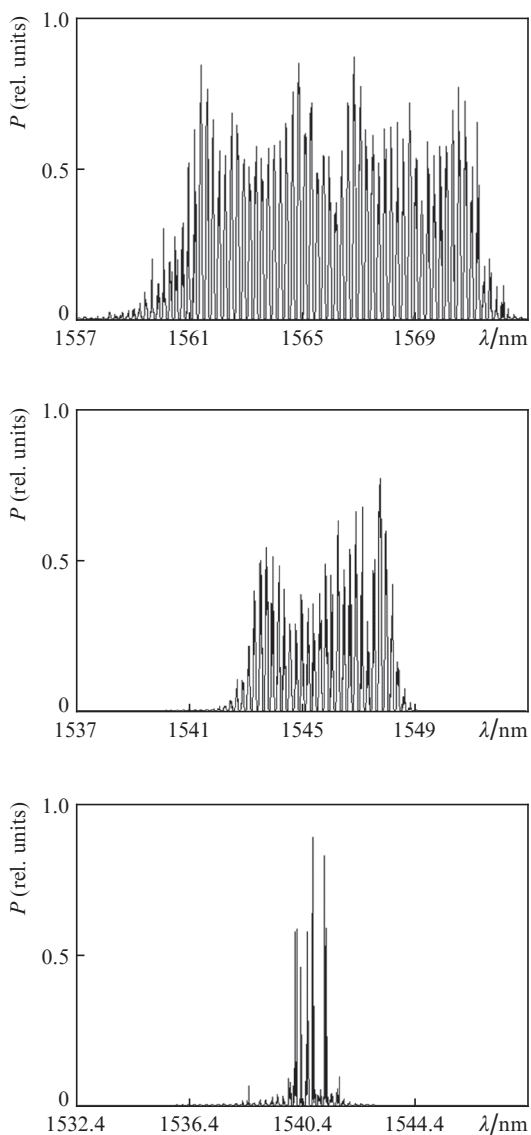


Figure 5. Emission spectra of LDs with a cavity length of 1.6 mm in copper housings at powers of (a) 300, (b) 60, and (c) 5 mW.

The LD power can be considerably increased in lasers with mesa-stripe widths of 4–5 μm instead of 3 μm . The output power can be also increased by mounting LDs on F-mounts rather than on C-mounts [15].

2.3. Spectral characteristics of LDs

Below, we present the spectral characteristics only for LDs in copper housings 11 mm in diameter, because our setup did not allow measuring the spectra of LDs on C-mounts.

Figure 5 presents the experimental spectra of LDs with a cavity length of 1.6 mm at output powers of 300, 60, and 5 mW and a heat sink temperature of 20°C. It is seen that the wavelength and the spectral width of laser radiation increase with increasing output power.

The dependences of the mean laser wavelength, which corresponds to the centre wavelength of the spectra shown in Fig 5, on the pump current are given in Fig. 6 for LDs with cavity lengths of 1.0 and 1.6 mm. In both cases, the laser wavelength increases with increasing heat sink temperature and pump current. The dependences of the spectral width (at half maximum) of laser radiation on the heat sink temperature and pump current for these LDs are presented in Fig. 7, which shows that the spectral width increases with increasing pump current but only slightly changes with increasing heat sink temperature.

The dependences of the wavelength and spectral width of LDs with a cavity length of 2.2 mm on the pump current are similar to the dependences shown in Figs 6 and 7. Note also that an increase in the spectral width of radiation with increasing pump current was reported almost in all works on high-power LDs.

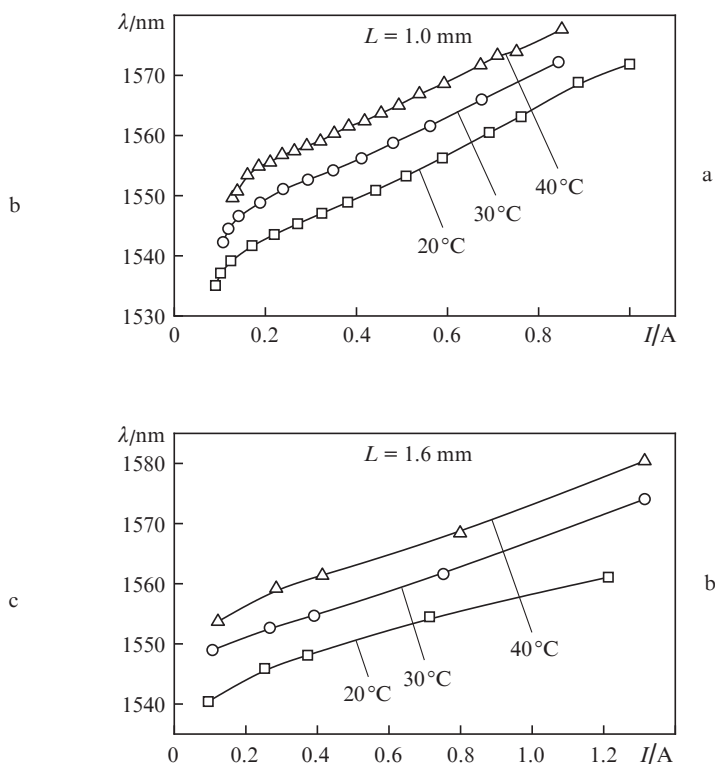


Figure 6. Dependences of the mean laser wavelength on the pump current for LDs (in copper housings) with cavity lengths of (a) 1 and (b) 1.6 mm.

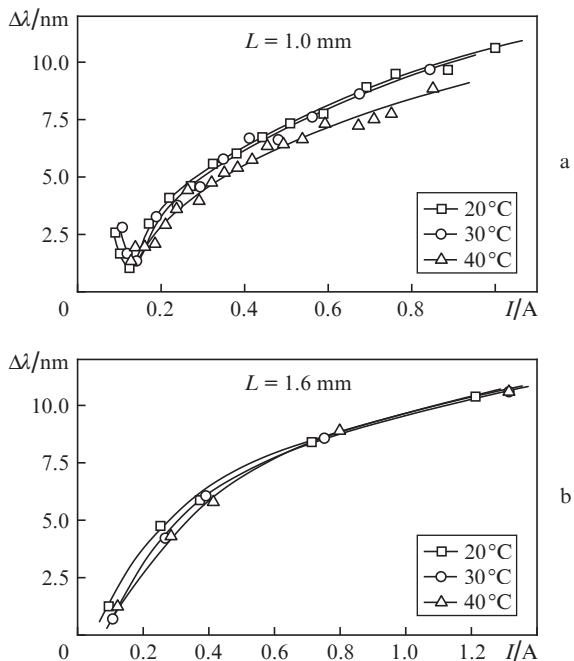


Figure 7. Dependences of the laser spectral width on the pump current for LDs (in copper housings) with cavity lengths of (a) 1 and (b) 1.6 mm.

2.4. Divergence and polarisation of LD radiation

In this work, we also studied the divergence of LD radiation along two mutually perpendicular axes at the 0.1 level and at half maximum of radiation intensity. Table 1 lists the divergences along the axes perpendicular (\perp) and parallel (\parallel) to the p–n junction for LDs with cavity lengths of 1.0, 1.6, and 2.2 mm at output powers $P = 50$ and 100 mW. One can see that the divergence along the axis parallel to the p–n junction increases with increasing power and decreases with increasing LD cavity length from 1.0 to 2.2 mm. The divergence along the axes perpendicular to the p–n junction does not depend on the output power and cavity length and is 44° – 46° at half maximum.

Almost the same results were obtained in work [1]. In this work, it was found that the width of the radiation pattern at half maximum increases insignificantly, from 8° near the lasing threshold to 9° at an output power of 185 mW. The measured far-field pattern in the plane perpendicular to the p–n junction testifies to generation of the fundamental optical mode. The divergence is 38° – 40° in the entire pump current range.

Following work [1], to confirm that the LD lasing in our study is single-mode, we measured the radiation pattern width

Table 1.

LD number	L/mm	P/mW	Radiation divergence/deg			
			level 0.1		level 0.5	
			\perp	\parallel	\perp	\parallel
16	1	50	93.4	16.6	44.5	6.9
		100	92.2	17.8	44.1	7.6
6	1.6	50	91	17	45.7	6.7
		100	86	18	44.5	7.5
12	2.2	50	100	14.7	45	5.1
		100	100	16.2	45	5.9

along the axis parallel to the p–n junction. The beam divergence of the LD with a cavity length of 1.6 mm and a mesa-stripe width of $3 \mu\text{m}$ was 6.7° at a laser power of 5 mW, 7.1° at 60 mW, 7.5° at 100 mW, 8.7° at 200 mW, and 12° at 300 mW. However, these data are insufficient to unambiguously conclude whether the radiation is single mode in the whole power range. Because of this, we assembled an optical transmitting module (POM) in a standard 14 pin DIL package, which was used for data transfer in fibre-optic communication lines with a single-mode fibre-optic cable (FOC). The dot-and-dash curve in Fig. 2b shows the P – I characteristic at the POM exit. The power at the FOC exit exceeded 100 W at a pump current $I > 650$ mA. Taking into account that 50% of radiation is lost when it is coupled into the FOC, the LD power was higher than 200 W. At $I > 700$ mA, the electronic temperature stabilisation circuit failed to remove heat from the thermoelectric cooler and switched off the POM. Thus, it was experimentally proved that the single-mode LD power was no lower than 200 mW.

Measurements showed that the LD radiation is strongly polarised. Table 2 presents the measured values of $\eta = (P_{\text{max}} - P_{\text{min}})/(P_{\text{max}} + P_{\text{min}})$ and $K = P_{\text{max}}/P_{\text{min}}$ for LDs with cavity lengths of 1.0, 1.6, and 2.2 mm for output powers $P = 50$ and 100 mW (P_{max} and P_{min} are the maximum and minimum powers at the exit of the polariser for its two mutually perpendicular positions).

The data of Table 2 show that the ratio of the TE-polarised radiation power to the TM-polarised power may exceed 700.

Table 2.

LD number	L/mm	P/mW	P_{max}/mW	$P_{\text{min}}/\mu\text{W}$	η	K
16	1	50	14.38	52	0.99	277
		100	29.98	40	0.997	749
6	1.6	50	15.48	57	0.993	271
		100	31.38	69	0.996	455
12	2.2	50	14.38	62	0.991	231
		100	29.58	130	0.991	228

2.5. Internal optical losses in the LDs

Important parameters for achieving high LD power and efficiency are internal optical losses α and injection efficiency η_{in} , which are determined from the relation [16, 17]

$$\frac{\hbar\omega}{q\eta_{\text{t}}} = \frac{1}{\eta_{\text{in}}}\left(1 + \frac{\alpha}{\alpha_{\text{m}}}\right), \quad (1)$$

where η_{t} is the power–current efficiency, $\alpha_{\text{m}} = L^{-1} \ln(1/\sqrt{R_1 R_2})$, L is the LD cavity length, R_1 and R_2 are the reflectivities of mirrors, $\hbar\omega$ is the photon energy, and q is the electron charge.

Figure 8 shows the dependence of η_{t}^{-1} on $1/\alpha_{\text{m}}$ for LDs with cavity lengths of 1.0, 1.6, and 2.2 mm, $R_1 = 100\%$, and $R_2 = 5\%$, which were mounted in copper housings 11 mm in diameter (the obtained results are independent of the type of mounting). The approximating straight line, which allowed us to determine $\alpha = 3.3 \text{ cm}^{-1}$ and $\eta_{\text{in}} = 0.7$, was drawn using the least-squares method.

In the present work, the value of α obtained for two QWs is 3.3 cm^{-1} . In work [1], these losses for the InGaAsP/InP system with two QWs were $\alpha = 5$ – 7 cm^{-1} for all the studied series of HSs. In [2], parameter α for the AlInGaAs/InP system for

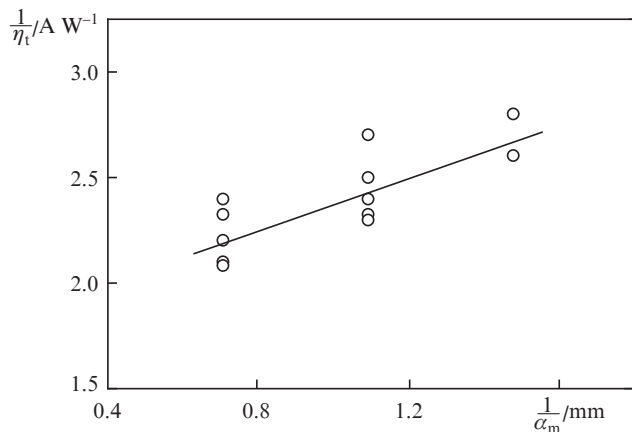


Figure 8. Dependence of the reciprocal power–current efficiency on the value $1/\alpha_m = L[\ln(1/\sqrt{R_1 R_2})]^{-1}$ for LDs with cavity lengths $L = 1.0$, 1.6 , and 2.2 mm.

radiation with $\lambda = 1.2\text{--}1.5$ μm was 8 cm^{-1} for four QWs and 12 cm^{-1} for six QWs.

3. Determination of characteristic temperatures of LDs

To determine the characteristic temperatures of the LDs, let us use the results of work [17]. The LD power was calculated by the formula

$$P = \eta_t(I, P, \Delta T)[I - I_t(I, P, \Delta T)]. \quad (2)$$

The dependences of the threshold current I_t and power–current efficiency η_t on the pump current, output power, and temperature can be represented in the form

$$I_t(I, P, \Delta T) = I_{t0} \exp\left(\frac{\Delta T_{id}(I, P, \Delta T)}{T_i}\right), \quad (3)$$

$$\eta_t(I, P, \Delta T) = \eta_{t0} \exp\left(\frac{-\Delta T_{id}(I, P, \Delta T)}{T_p}\right), \quad (4)$$

where I_{t0} and η_{t0} are the threshold current and power–current efficiency without taking into account heating of the LD active region, T_i and T_p are the characteristic temperatures of the LD for the threshold pump current and the power–current efficiency.

The change in the active region temperature due to heating is written as

$$\Delta T_{id}(I, P, \Delta T) = R_{T0} \left(\frac{T_0 + \Delta T_{id}(I, P, \Delta T)}{T_0} \right)^k (UI - P) + \Delta T, \quad (5)$$

where $T_0 = 293$ K and $\Delta T = 0, 10$, and 20 K. The LD temperature $T = T_0 + \Delta T$ was kept constant at $20, 30$, and 40 °C using an electronic stabilisation circuit.

One of the main parameters that determine the maximum LD output power is its thermal resistance. The thermal resistance of the interface between the active region and the contact plate was calculated by the formula [18]

$$R_{id} = \frac{1}{k_T \pi L} \ln\left(\frac{16h_{ld}}{\pi w}\right), \quad (6)$$

where k_T is the thermal conductivity, h_{ld} is the LD crystal height, and w is the mesa-stripe width. The thermal conductivity k_T of the InP crystal was taken to be $0.68\text{ W (cm} \cdot \text{K)}^{-1}$, and k_T for the $\text{Al}_x\text{Ga}_y\text{In}_{1-x-y}\text{As}$ structure was $0.05\text{--}0.07\text{ W (cm K)}^{-1}$ depending on x at $1-x-y = 0.52$ [19, Fig. 2.34].

The thermal resistance of the interface between the active region and the heat sink, which was used in calculations, was determined as $R_{T0} = R_{id} + R_{rad}$, where R_{rad} is the thermal resistance of the heat sink (together with the LD mount). The value $R_{rad} = 4.8\text{ K W}^{-1}$ for LDs in copper housings was borrowed from [17]. In calculations for LDs with $w = 3$ μm and $h_{ld} = 100$ μm , we used $R_{T0} = 32\text{ K W}^{-1}$ at $L = 1.0$ mm, $R_{T0} = 21\text{ K W}^{-1}$ at $L = 1.6$ mm, and $R_{T0} = 17\text{ K W}^{-1}$ at $L = 2.2$ mm.

Asterisks in Fig. 1b indicate the calculated powers of radiation from the antireflection-coated faces of laser diodes with a cavity length of 1.0 mm in copper housings. The best coincidence between the experimental and calculated data in this case is observed at $T_i = 70$ K, $T_p = 190$ K, $I_{t0} = 0.072$ A, $\eta_{t0} = 0.45\text{ W A}^{-1}$, and $k = 1.7$.

Asterisks in Fig. 2b indicate the calculated powers of radiation from the antireflection-coated faces of LDs with a cavity length of 1.6 mm in copper housings. The best coincidence between the experimental and calculated data in this case is observed at $T_i = 80$ K, $T_p = 280$ K, $I_{t0} = 0.08$ A, $\eta_{t0} = 0.35\text{ W A}^{-1}$, and $k = 1.4$.

Analysis of our calculations leads to the following conclusions: the characteristic temperature T_i changes within the range of $70\text{--}80$ K, while the characteristic temperature T_p changes from 190 to 280 K. In [17], the characteristic temperatures were determined to be $T_i = 53$ K and $T_p = 100$ K. The higher values of the characteristic temperatures obtained in our work are obviously explained by a closer position of the active region to the heat sink and by a more efficient heat removal than those in work [17], in which the thicknesses of the waveguiding layers were 0.65 and 1 μm .

4. Conclusions

It is shown that lasers with a cavity length of 1.6 mm and a mesa-stripe width of 3 μm soldered on a contact plate or mounted in a copper housing 11 mm in diameter can emit radiation with a power exceeding 300 mW. The output power of lasers on C-mounts may reach 400 mW and more. When mounting lasers in a standard 14 pin DIL package, one can obtain a power no lower than 100 mW at the exit from a single-mode cable, which, taking into account 50% losses of radiation upon its coupling into the FOC, corresponds to the single-mode LD power exceeding 200 mW.

References

1. Leshko A.Yu., Lyutetskii A.V., Pikhtin N.A., Slipchenko S.O., et al. *Semiconductors*, **36**, 1308 (2002) [*Fiz. Tekh. Poluprovodn.*, **36**, 1393 (2002)].
2. Slipchenko S.O., Lyutetskii A.V., Pikhtin N.A., et al. *Pis'ma Zh. Tekh. Fiz.*, **29**, 65 (2003).
3. Sokolova Z.N., Tarasov I.S., Asryan L.V. *Semiconductors*, **46**, 1044 (2012) [*Fiz. Tekh. Poluprovodn.*, **46**, 1067 (2012)].
4. Lysevych M., Tan H.H., Karouta F., Jagadish C. *Opt. Express*, **22**, 8156 (2014).
5. Tarasov I.S. *Quantum Electron.*, **40**, 661 (2010) [*Kvantovaya Elektron.*, **40**, 661 (2010)].
6. Slipchenko S.O., Vinokurov D.A., Pikhtin N.A., et al. *Semiconductors*, **38**, 1430 (2004) [*Fiz. Tekh. Poluprovodn.*, **38**, 1477 (2004)].

7. Lyutetskii A.V., Borshchev K.S., et al. *Semiconductors*, **42**, 104 (2008) [*Fiz. Tekh. Poluprovodn.*, **42**, 106 (2008)].
8. Kabanov V.V., Lebiadok U.V., Ryabtsev G.I., et al. *Semiconductors*, **46**, 1316 (2012) [*Fiz. Tekh. Poluprovodn.*, **46**, 1339 (2012)].
9. Makino T., Evans J.D., et al. *Appl. Phys. Lett.*, **71**, 2871 (1997).
10. Elenkrig B.B., Smetona S., Simmons J.G., et al. *Appl. Phys.*, **85**, 2367 (1999).
11. Ryvkin B.S., Avrutin E.A. *Appl. Phys.*, **97**, 113106 (2005).
12. Ryvkin B.S., Avrutin E.A. *Appl. Phys.*, **101**, 123115 (2007).
13. Veselov D.A., Shashkin I.S., Bakhvalov K.V., et al. *Semiconductors*, **50**, 1225 (2016) [*Fiz. Tekh. Polupr.*, **50**, 1247 (2016)].
14. Elenkrig B.B., Smetona S., Simmons J.G., et al. *Appl. Phys.*, **87**, 1 (2000).
15. Bezotosnyi V.V., Krokhin O.N., Oleshchenko V.A., et al. *Quantum Electron.*, **45**, 1088 (2015) [*Kvantovaya Elektron.*, **45**, 1088 (2015)].
16. Zhukov A.E. *Lasery na osnove poluprovodnikovyykh nanostruktur* (Lasers Based on Semiconductor Nanostructures) (St. Petersburg: Elmor, 2007).
17. Gorlachuk P.V., Ivanov A.V., Kurnosov V.D., Kurnosov K.V., et al. *Quantum Electron.*, **44**, 149 (2014) [*Kvantovaya Elektron.*, **44**, 149 (2014)].
18. Amann M.-C. *Appl. Phys. Lett.*, **50**, 4 (1987).
19. Adachi S. *Properties of Semiconductor Alloys: Group-IV, III–V and II–VI Semiconductors* (John Wiley & Sons, 2009).